Solar Energy Materials & Solar Cells 140 (2015) 92–100

Contents lists available at ScienceDirect

Solar Energy Materials & Solar Cells

journal homepage: www.elsevier.com/locate/solmat

Physics of the temperature coefficients of solar cells

O. Dupré [a,b,*], R. Vaillon [a], M.A. Green [b]

[a] Université de Lyon, CNRS, INSA – Lyon, UCBL, Centre for Energy and Thermal Sciences (CETHIL), UMR5008, F-69621 Villeurbanne, France
[b] Australian Centre for Advanced Photovoltaics (ACAP), School of Photovoltaic and Renewable Energy Engineering, University of New South Wales, Sydney 2052, Australia

ARTICLE INFO

Article history:
Received 9 January 2015
Received in revised form
27 February 2015
Accepted 20 March 2015

Keywords:
Temperature coefficient
Solar cell
Generation–recombination
Open circuit voltage
External Radiative Efficiency

ABSTRACT

Physics ruling the temperature sensitivity of photovoltaic (PV) cells is discussed. Dependences with temperature of the fundamental losses for single junction solar cells are examined and fundamental temperature coefficients (TCs) are calculated. Impacts on TCs of the incident spectrum and of variations of the bandgap with temperature are highlighted. It is shown that the unusual behavior of the bandgaps of perovskite semiconductor compounds such as $CH_3NH_3PbI_{3-x}Cl_x$ and $CsSnI_3$ will ultimately, in the radiative limit, give PV cells made of these materials peculiar temperature sensitivities. The different losses limiting the efficiency of present commercial cells are depicted on a p–n junction diagram. This representation provides valuable information on the energy transfer mechanisms within PV cells. In particular, it is shown that an important fraction of the heat generation occurs at the junction. A review of the loss mechanisms driving the temperature coefficients of the different cell parameters (open circuit voltage V_{oc}, short circuit current density J_{sc}, fill factor *FF*) is proposed. The temperature sensitivity of open circuit voltage is connected to the balance between generation and recombination of carriers and its variation with temperature. A general expression that relates the temperature sensitivity of V_{oc} to the External Radiative Efficiency (ERE) of a solar cell is provided. Comparisons with experimental data are discussed. The impacts of bandgap temperature dependence and incident spectrum on the temperature sensitivity of short circuit current are demonstrated. Finally, it is argued that if the fill factor temperature sensitivity is ideally closely related to the open circuit voltage temperature sensitivity of the cell, it depends for some cells strongly on technological issues linked to carrier transport such as contact resistances.

1. Introduction

It has long been observed that temperature affects negatively the performances of photovoltaic (PV) devices [1,2]. This is an important issue for the PV industry because the efficiency of PV modules is lower under real operating conditions than under Standard Test Conditions (STC) and because it increases the difficulty in predicting PV energy production.

Several articles have investigated the theoretical temperature dependences of solar cell output parameters [1–9]. The analyses provided important information on the general trends of the temperature behavior of solar cells explaining for example the small temperature sensitivity of cells with large bandgaps. However, the use of one or several semi-empirical parameters to calculate the diode current restricted the generality of the conclusions and in some cases led to systematic errors in modeling as demonstrated elsewhere [10]. Identifying the different mechanisms driving the temperature sensitivity of solar cells, Green derived some general equations for temperature coefficients from internal device physics [10]. Siefer and Bett [11] made theoretical calculations illustrating that temperature coefficients are function of the dominant recombination processes. Recently, a group from NREL observed experimentally that metastable changes due to light exposure modify the temperature dependence of the fill factor of CIGS thin film cells [12]. Their analysis illustrates the depth of the correlation between device physics and temperature coefficients.

This paper investigates the physics that governs the temperature behavior of solar cells. First, building on the work of Hirst and Ekins-Daukes [13], the temperature dependences of the "fundamental" losses in photovoltaic conversion are discussed. Then, the analysis is extended to additional losses such as non-radiative recombinations in order to explain the physics behind the temperature coefficients of real devices. Finally, the different mechanisms driving the temperature sensitivity of open circuit voltage (V_{oc}), short circuit current (J_{sc}) and fill factor (*FF*) are discussed.

* Corresponding author. Tel.: +33 4 72 43 74 20.
E-mail address: olivier.dupre@insa-lyon.fr (O. Dupré).

http://dx.doi.org/10.1016/j.solmat.2015.03.025
0927-0248/

2. Fundamental losses in photovoltaic conversion

2.1. Detailed balance principle and thermodynamics

Fundamentally, photovoltaic devices are energy converters that turn thermal energy from the sun into electrical energy. This means that a solar cell, like any heat engine, is ultimately limited by the Carnot efficiency [14,15]. However, even ideal PV devices differ from Carnot engines because the energy exchanged is radiative and because the energy emitted by the devices is considered a loss in PV conversion since the hot reservoir is the Sun. Moreover, typical PV cells absorb solar photons from a small solid angle while they emit in a much broader solid angle. Additionally, for typical single junction cells, there is an important loss due to the spectral mismatch between the incident radiation and the absorption in the cell that generates electrical carriers.

Hirst and Ekins-Daukes derived from the detailed balance principle [16] an approximate relation between a PV cell bandgap (E_g) and its voltage at maximum power point (V_{MPP}) [13]:

$$qV_{MPP} \approx E_g\left(1 - \frac{T_c}{T_s}\right) - kT_c \ln\left(\frac{\Omega_{emit}}{\Omega_{abs}}\right) \quad (1)$$

q, k, T_c and T_s, Ω_{abs} and Ω_{emit} are respectively the electron charge, Boltzmann's constant, the cell and sun temperatures, the absorption and emission solid angles. Interestingly, this equation displays classical thermodynamic terms. The first term on the right hand side contains the Carnot efficiency which expresses the necessity of evacuating the incoming entropy. The second term on the right hand side is the voltage loss related to the entropy generated due to the solid angle mismatch between absorption and emission.

The current density at maximum power point J_{MPP} is given by

$$J_{MPP} = q(n_{abs} - n_{emit}(V_{MPP})) \quad (2)$$

where n_{abs} and n_{emit} are the photon absorption and emission rates given by the generalized Planck's equation [17]:

$$n_{abs}(E_g, T_s, \Omega_{abs}) = \frac{2\,\Omega_{abs}}{c^2\,h^3}\int_{E_g}^{\infty}\frac{E^2}{e^{\frac{E}{kT_s}} - 1}\,dE \quad (3)$$

$$n_{emit}(E_g, V, T_c, \Omega_{emit}) = \frac{2\,\Omega_{emit}}{c^2\,h^3}\int_{E_g}^{\infty}\frac{E^2}{e^{\frac{E-qV}{kT_c}} - 1}\,dE \quad (4)$$

where c and h are the speed of light in vacuum and Planck's constant, respectively. Perfect charge transport is assumed so the free enthalpy of the photogenerated electron–hole pairs – namely the chemical potential μ of the electron–hole system [18] – is equal to qV where V is the voltage across the cell terminals.

Table 1 shows the analytical expressions, similar to that in Ref. [13], of the energy losses related to the effects mentioned previously. These loss mechanisms are depicted in Fig. 1 which shows how the energy of the incident photons is converted within an ideal p–n junction solar cell. The first two losses are related to the spectral mismatch between the broadband incident radiation and the spectrally limited cell absorption: (1) some photons have more energy than E_g and this "extra" energy is quickly lost by the excited electrons to the lattice atoms in a process called thermalization and (2) some photons have less energy than E_g and are not able to excite any electron ("below E_g" loss). The last three losses impact the balance between absorption and emission rates; we will call them in the following "balance losses". The emission term limits the cell current and corresponds to the energy of the emitted photons at MPP. The Carnot and angle mismatch terms represent the energy lost because of the voltage drop at the junction necessary to efficiently collect the excited charges (illustrated in Fig. 1). Physically, all the charges that go through the junction are accelerated by the electric field and gain some kinetic energy at the expense of a fraction of their potential energy. Then, they quickly relax to the potential energy of the conduction band of the other side through collisions with the lattice atoms. This heat generation process can be identified as Peltier heating [19]. This phenomenon, rarely reported in the PV literature, means that a large part of the heat generation in PV cells is located at the junction. In most PV cells, the p–n junction is located near the front of the cell. High energy photons which contribute to most of the heat generation by thermalization also happen to be absorbed near the front of the cell.

Fig. 1 illustrates that some losses limit the voltage of the cell while others limit its current. This is why angle mismatch, Carnot and emission losses are distinguished even though they stem from the same physical mechanism: radiative recombination. In fact, any recombination process has this dual impact: (1) a current loss because some excited charges don't make it to the external circuit

Table 1
Fundamental losses in a single junction solar cell.

Spectral mismatch	Thermalization	$\frac{2\,\Omega_{abs}}{c^2\,h^3}\int_{E_g}^{\infty}\frac{E^2}{e^{\frac{E}{kT_s}} - 1}(E - E_g)dE$	(5)
	Below E_g	$\frac{2\,\Omega_{abs}}{c^2\,h^3}\int_{0}^{E_g}\frac{E^2}{e^{\frac{E}{kT_s}} - 1}E\,dE$	(6)
Absorption–emission balance	Emission	$E_g\frac{2\,\Omega_{emit}}{c^2\,h^3}\int_{E_g}^{\infty}\frac{E^2}{e^{\frac{E-qV_{MPP}}{kT_c}} - 1}dE$	(7)
	Angle mismatch	$kT_c \ln\left(\frac{\Omega_{emit}}{\Omega_{abs}}\right)J_{MPP}$	(8)
	Carnot	$E_g\left(\frac{T_c}{T_s}\right)J_{MPP}$	(9)

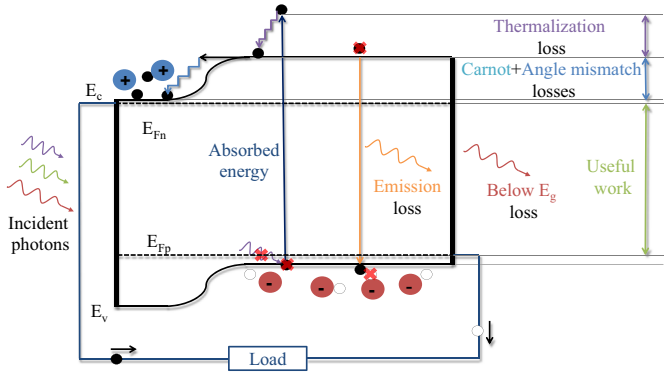

Fig. 1. Fundamental loss mechanisms illustrated on a p–n junction diagram. E_c, E_v are the energies of the bottom edge of the conduction band and the top edge of the valence band, respectively. E_{Fn} and E_{Fp} are the quasi Fermi levels of electrons and holes, respectively.

and (2) a voltage loss because the generation–recombination balance is diminished thus reducing the voltage that can build in the cell.

Eq. (4) shows that radiative emission increases with cell temperature. This is the consequence of increased recombination rate at larger temperature due to the augmentation of the equilibrium carrier concentration. This leads to a negative temperature sensitivity of the absorption–emission rate balance that is the origin of the temperature behavior of PV cells and explains why all PV devices become less efficient as they heat up. A thermodynamical viewpoint is that maximum efficiency decreases with temperature because it requires more energy to evacuate entropy in an environment at larger temperature.

Fig. 2 shows the temperature dependence of the previously discussed "fundamental losses". In this simplistic case, only the "balance losses" are sensitive to temperature. On the temperature range of PV device operation, their variations with temperature are approximately linear. This explains the generally observed linear behavior of the output power. For that reason, temperature sensitivities of solar cell are often described by a single value of temperature coefficient (TC). TCs are usually defined normalized at 25 °C [20] and expressed in ppm K^{-1}:

$$\beta_G(T_c) = \frac{10^6}{G(298.15\ \mathrm{K})}\frac{G(T_c) - G(298.15\ \mathrm{K})}{T_c - 298.15} \tag{10}$$

where G is the parameter of interest. If the variation is linear with temperature, β_G is well described by a single value.

Using Boltzmann's approximation in Eq. (7) and neglecting $2E_gkT_c+2k^2T_c^2$ in front of E_g^2 in the integration by parts results in a linear approximation of the "Emission" loss term:

$$\text{Emission} \approx \left(E_g^3\frac{2\Omega_{emit}}{c^2h^3}k\, e^{-\frac{E_g}{kT_s}-\ln\left(\frac{\Omega_{emit}}{\Omega_{abs}}\right)}\right)T_c \tag{11}$$

Neglecting the temperature variation of J_{MPP}, Eqs. (8) and (9) indicate that the "angle mismatch" and "Carnot" losses also vary linearly with temperature. These approximations enable to find an estimate of the temperature coefficient of the maximum efficiency as a function of the balance losses at a reference temperature:

$$\beta_{\eta\ max} \approx \frac{10^6}{P_{max}(298.15\ \mathrm{K})}\frac{-\text{balance losses}\ (298.15\ \mathrm{K})}{298.15} \tag{12}$$

Because temperature coefficients are normalized, any mechanism impacting the efficiency of the cell modifies its temperature coefficient. The approximate expression in Eq. (12) emphasizes that temperature sensitivity is mainly a function of the generation–recombination balance of the cell. It was observed long ago that the temperature sensitivity of device performance improves together

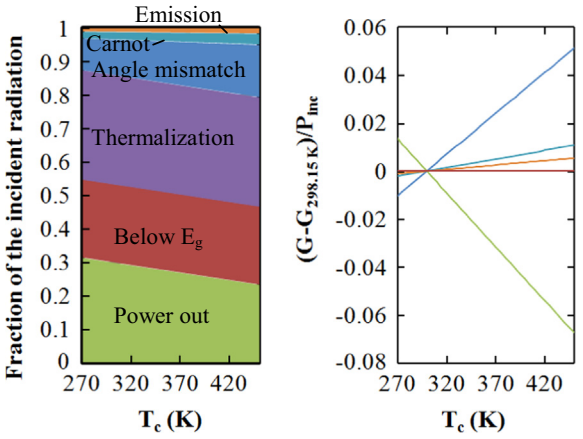

Fig. 2. Temperature dependences of the fundamental losses (Table 1) for a bandgap of 1.12 eV (E_g of c-Si at 298.15 K).

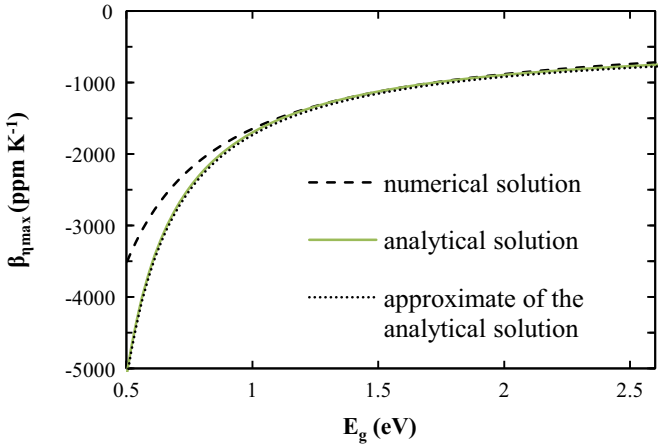

Fig. 3. Fundamental temperature coefficient of the maximum efficiency of photovoltaic cells as a function of bandgap.

with open circuit voltage [3]. This is due to the fact that the open circuit voltage of the cell is a good indicator of the generation–recombination balance. One way of improving this balance is by concentrating more light upon the cell; this is known to increase V_{oc} and reduce temperature sensitivity [8,21]. Another way of changing this balance is by modifying non-radiative recombination (NRR) rates. In Section 3, we will consider NRRs and analyze how they impact temperature coefficients.

Fig. 3 shows the "fundamental temperature coefficient" of PV cells calculated with different approximations. The numerical solution corresponds to the resolution of the ideal diode equation in the Shockley–Queisser limit [16]. The analytical solution based on [13], Eqs. (1) and (2), and its approximation, Eq. (12), provide a good estimate of temperature coefficients as long as E_g is not too small. One can observe that the absolute value of the temperature coefficient is larger for smaller bandgaps. This is because temperature coefficients are normalized values that are mainly driven by the open circuit voltage (see Section 3.1 or Ref. [10]).

2.2. Bandgap temperature dependence and influence of the incident spectrum

All the fundamental losses in PV conversion are function of the bandgap (Table 1). Fig. 3 shows the temperature coefficient of maximum efficiency at different bandgaps with a simplistic assumption. In practice, the bandgaps of semiconductors change substantially with temperature. These variations are due to modifications of the

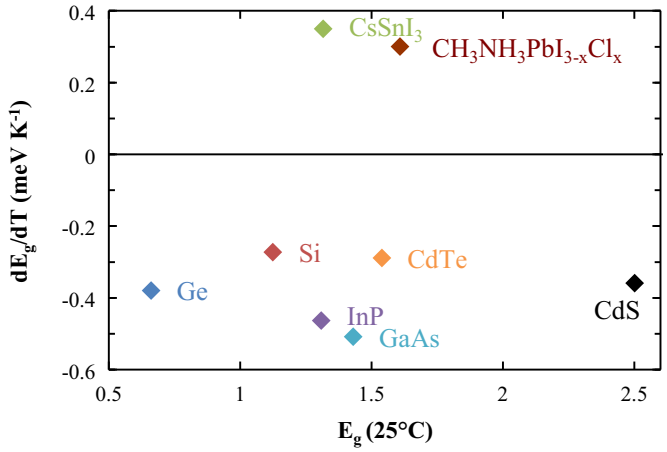

Fig. 4. Slope of the linear approximation of bandgap temperature dependence around 300 K. $E_g=f(T)$ from Ref. [25], from Ref. [26] for Si, from Ref. [23] for $CsSnI_3$, and from Ref. [24] for $CH_3NH_3PbI_{3-x}Cl_x$.

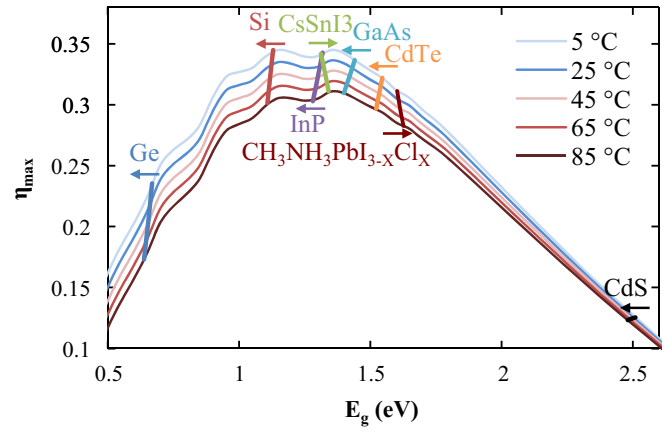

Fig. 5. Shockley–Queisser limit and maximum theoretical efficiencies of several semiconductors at different temperatures.

band energies caused by electron–phonon interactions and by thermal expansion of the lattice [22]. Most semiconductor bandgaps decrease almost linearly in the temperature range of operation of PV cells [23]. However, there is no general relation between bandgap and temperature dependence of bandgap as shown in Fig. 4. There are some exceptions where bandgap actually increases with temperature and of particular interest for photovoltaics are the perovskite semiconductor compounds $CsSnI_3$ and $CH_3NH_3PbI_{3-x}Cl_x$ [23,24]. It is likely that related perovskite compounds also have such unusual bandgap temperature dependences.

These bandgap temperature dependences impact directly the temperature coefficients and also create an influence of the incident spectrum on TCs as can be observed in Figs. 5 and 6. Fig. 5 shows the "Shockley–Queisser efficiency limit" calculated with the latest AM1.5 spectrum [27] at different temperatures. The maximum efficiencies of different semiconductors are plotted using their bandgap temperature dependences. Fig. 6 shows the TCs of these materials together with extrapolations of $TC=f(E_g)$ assuming different values of dE_g/dT. The green and blue extrapolated curves show opposite fluctuations because they assume bandgaps variations with temperature of opposite signs. These variations due to the incident spectrum are analyzed in more details in Section 3.2. Interestingly, while their bandgaps at room temperature are similar, $CsSnI_3$ will ultimately, i.e. in the radiative limit, be less temperature sensitive than InP because of the unusual behavior of its bandgap. On the other hand one can see that PV cells made of

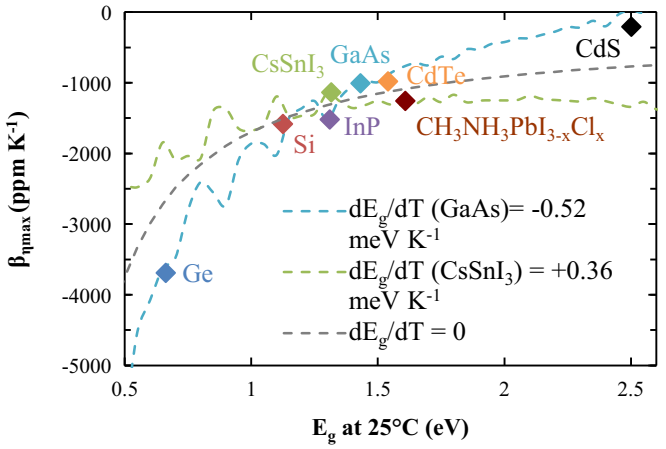

Fig. 6. Temperature coefficients of several semiconductors and extrapolations using different values of dE_g/dT. (For interpretation of the references to color in this figure, the reader is referred to the web version of this article.)

$CH_3NH_3PbI_{3-x}Cl_x$ will, in the radiative limit, suffer more severely from heat than cells made of other semiconductors with similar bandgaps. Indeed, it appears that the impact of dE_g/dT on TC is function of $d\eta/dE_g$ and thus depends on E_g and the incident spectrum. It is of particular importance for semiconductors whose bandgaps are away from the optimum such as top and bottom cells of multijunction PV cells. Some works [22,28] indicate that the bandgap temperature dependence of certain quantum dots change with their sizes. This indicates a potential way of tuning dE_g/dT to optimize the TC of future PV cells.

One should note that this analysis in the radiative limit (where radiative recombination dominates non-radiative recombination processes such as Auger or Shockley Read Hall) does not give the theoretical minimum of temperature coefficients. Among the additional losses, some may decrease with temperature (series resistance for example). This can lead to temperature coefficients of lower magnitudes as sometimes observed for newly-developed technologies [10]. However, temperature coefficients are expected to converge toward these values as technologies improve towards the radiative limit. To be more accurate in determining ultimate values, one should account for Auger recombination which is also an intrinsic limiting mechanism. Using the state-of-the-art parameters [29] and considering carefully their temperature dependences, we derived the temperature coefficient of the limiting efficiency of crystalline silicon solar cells. The result is -2380 ppm K^{-1} which is significantly larger than the value in the radiative limit (-1582 ppm K^{-1}). As discussed above this does not correspond to a minimum, but, as the devices improve, the temperature sensitivities of crystalline silicon solar cells are expected to converge towards this value.

3. Additional losses in real devices

Present commercial photovoltaic cells have efficiencies considerably lower than the Shockley–Queisser limit defined by the fundamental losses described previously. In this section, the additional losses limiting real device performances are introduced and their impacts on temperature coefficients are analyzed.

Fig. 7 shows the band diagram of a realistic solar cell operating at its Maximum Power Point (MPP). The most important losses stem from the non-radiative recombinations (NRR). The different NRR processes (Shockley Read Hall, Auger, surface) are illustrated. Other losses include reflection at the front of the cell, electrical shunts, imperfect contacts and finite mobilities of the carriers. Transmission losses (i.e. photons with sufficient energy but that are not absorbed) are not

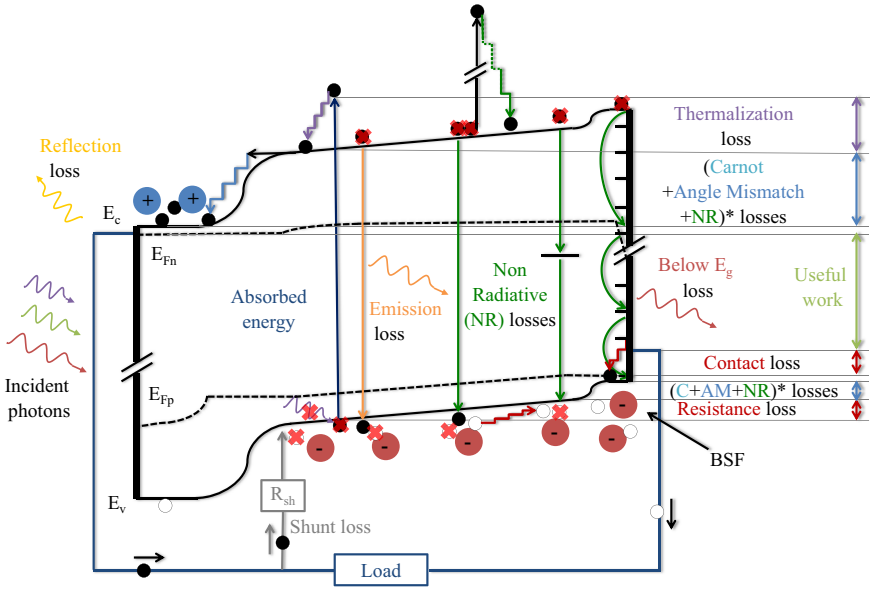

Fig. 7. Conversion loss mechanisms of a PV cell illustrated on a p–n junction diagram.

depicted here but can reduce the efficiency of thin PV cells with insufficient light trapping. The representation of Fig. 7 is interesting in that it shows where and how the different energy losses happen. For example, the "resistance loss" corresponds to the kinetic energy lost by the charges to the semiconductor atoms during collisions along their paths.

As in Fig. 1, we observe in Fig. 7 that mechanisms reducing the generation–recombination balance result in a voltage loss, which occurs at the interfaces with the selective membranes that force the photogenerated charges in opposite directions. In this example, it occurs at the p–n junction and also slightly in the region of the back surface field (BSF). For other configurations it could be different (e.g. pin structure consists in two separate junctions). Reflection, transmission and shunts, similarly to every current losses, also add to this voltage drop but their contribution is usually negligible so it is not depicted in Figs. 7 and 8.

In Fig. 8, the IV curve of the cell is depicted together with the different losses at the MPP. By identifying the voltage and current losses, it is possible to understand the shape of the current-voltage characteristic. Note that the reflection loss in standard c-Si PV devices is much lower because their front surface is usually texturized (often with random pyramids). For the sake of illustration, it is the photon flux density absorbed by a planar cell (calculated with OPALv1.3 [30]) that is plotted.

Since the PV cell parameters (V_{oc}, I_{sc}, FF) usually vary approximately linearly with temperature, it is possible to separate the temperature sensitivity of the device performance into the sum of their temperature coefficients:

$$P_{max}(T_c) = V_{oc}(T_c)\ J_{sc}(T_c)\ FF(T_c)$$

$$\beta_{P_{max}} = \beta_{V_{oc}} + \beta_{J_{sc}} + \beta_{FF} \quad (13)$$

where P_{max} is the maximum power by unit area. This is particularly interesting because these different TCs depend on different loss mechanisms.

3.1. Open circuit voltage temperature sensitivity

The temperature sensitivity of open circuit voltage is of particular importance since it accounts for 80–90% of the overall temperature sensitivity for reasonably good solar cells [10].

The open circuit voltage of a solar cell corresponds to the state where the total rate of photogeneration equals that of recombination

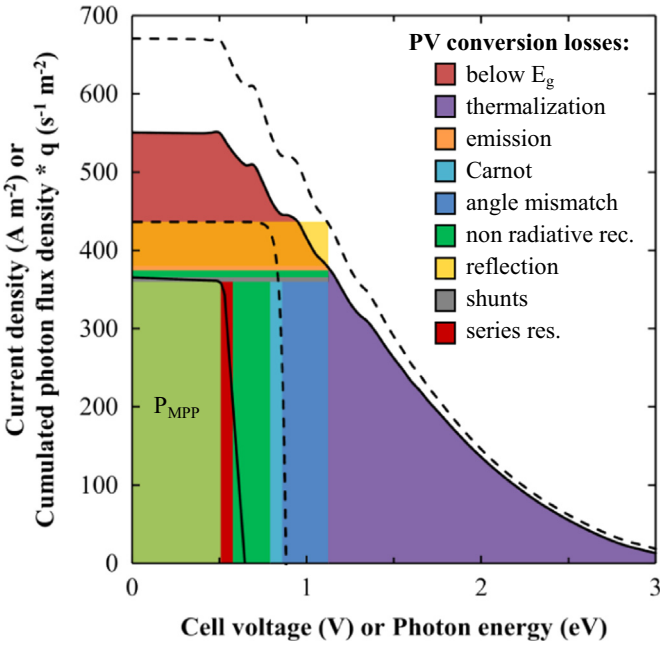

Fig. 8. Conversion loss mechanisms of a c-Si cell at MPP. Cumulated photon flux density of the AM1.5 spectrum (dashed line), of the transmitted fraction of this radiation perpendicularly incident through a planar c-Si surface (solid line). Ideal IV characteristic (dashed line) and IV characteristic of a c-Si PV cell with a planar surface (solid line). Note that this kind of graph was first introduced by Hirst and Ekin Daukes in the radiative limit [13]. (For interpretation of the references to color in this figure legend, the reader is referred to the web version of this article.)

so that no current circulates through the circuit. Its relative change with temperature, β_{Voc}, is thus an indication of the temperature dependence of the generation–recombination balance. The photogeneration rate is a function of incident spectrum, concentration, reflection, transmission and parasitic absorption. The recombination rate depends on the importance of the different recombination processes (radiative, Shockley Read Hall, Auger, surface, shunts).

Recognizing that every recombination mechanism is a function of the product of the local hole and electron concentrations np, Green derived a general expression for the temperature sensitivity of V_{oc} (Eq. (13) in Ref. [10]). This formula, derived from the basis of internal device physics, is always valid but requires the detailed

knowledge of the recombination mechanisms in the cell of interest. On the other hand, Braun et al. proposed an approximate formulation for dV_{oc}/dT in the radiative limit for concentrator solar cells (Eq. (7) in Ref. [21]). We show in the following that it can be written more simply in a form similar to the general expression derived by Green and propose an extension, Eq. (18) with Eqs. (15) and (19), that goes beyond the radiative limit by using the concept of External Radiative Efficiency (ERE). The ERE of a PV cell is similar to the External Quantum Efficiency (EQE) of a Light-Emitting Diode (LED). It is defined in Ref. [31] as "the fraction of the total dark current recombination in the device that results in radiative emission from the device". The output current and the open circuit voltage of the cell can thus be written as

$$J = XJ_{sc,1sun} - \frac{1}{ERE} J_{0,rad} e^{\frac{qV}{kTc}} \tag{14}$$

$$V_{oc} = \frac{kT_c}{q} \ln\left(\frac{X J_{sc,1sun}}{(1/ERE_{oc}) J_{0,rad}}\right) = V_{oc,1sun} + \frac{kT_c}{q}(\ln(ERE_{oc}) + \ln(X)) \tag{15}$$

Transport resistances are neglected, ERE_{oc} is the ERE at open circuit, X is the concentration factor and $J_{0,rad}$ is the dark current density in the radiative limit. Using the same approximations as for Eq. (11), we get

$$J_{0,rad} \approx q\frac{2\Omega_{emit}}{c^2h^3} kT_c E_g{}^2 e^{-\frac{E_g}{kTc}} \tag{16}$$

Assuming a linear variation of E_g on the temperature range of interest, i.e. dE_g/dT_c =cste, we use

$$E_g = E_{g0} + T_c \frac{dE_g}{dT_c} \tag{17}$$

By differentiating Eq. (15), the temperature dependence of V_{oc} becomes

$$\frac{dV_{oc}}{dT_c} = -\frac{\frac{E_{g0}}{q} - V_{oc} + \gamma\frac{kT_c}{q}}{T_c} \tag{18}$$

with

$$\gamma = 1 - \frac{d\ln ERE_{oc}}{d\ln T_c} + \left(2\frac{d\ln E_g}{d\ln T_c} - \frac{d\ln J_{sc,1sun}}{d\ln T_c}\right) \tag{19}$$

Eq. (18) predicts a temperature coefficient of the open circuit voltage approximately constant over the range of temperature typical of solar cell operation [10]. Eq. (18) is the same as in Ref. [2], but the coefficient γ is explicitly quantified in Eq. (19). As previously mentioned elsewhere [32], γ corresponds now explicitly to the temperature sensitivity of the mechanisms determining V_{oc}. The absolute value of the terms in parentheses in Eq. (19) is less than 0.5 for all the semiconductors considered here. Thus, it is $1-\frac{d\ln ERE_{oc}}{d\ln T_c}$ (quite similar to $\gamma\frac{f}{\xi}\frac{d\xi}{df}$ in Ref. [10]) that plays a major role in the value of γ. The temperature dependence of the ERE depends on the recombination mechanisms within the cell so γ gives an information on the dominant recombination processes. To illustrate this idea, the previous analysis is applied to two different situations using the same approximations as in Ref. [11]. If the dark saturation current is dominated by recombination within the space charge region (as is often the case at low injection levels [11]) with an ideality factor close to two, the term γ reads $5-2\frac{d\ln J_{sc}}{d\ln T_c} \approx 5$. If the dark saturation current is dominated by bulk and surface recombinations with an ideality factor close to unity, γ becomes $3-\frac{d\ln J_{sc}}{d\ln T_c} \approx 3$.

We calculated γ from experimental values of β_{Voc} for crystalline silicon cells [3,7,32]. The γ values range from 0 to 2. This demonstrates that there are other configurations than the two described above.

The most important term in dV_{oc}/dT_c and thus in β_{Voc} is $E_{g0}/q - V_{oc}$. However the term $\gamma kT_c/q$ is non-negligible in the determination of β_{Voc}. For example, it accounts for between 0% and 10% of β_{Voc} for the cells described in Refs. [3,7,32].

Practically, ERE_{oc} can be calculated from simple experimental measurements by using the reciprocity relation between External Quantum Efficiency and electroluminescent emission of solar cells [33]:

$$\mathrm{ERE}_{oc} = \frac{q\frac{2\Omega_{emit}}{c^2h^3}\int_0^\infty \frac{\overline{\mathrm{EQE}}\, E^2}{e^{\frac{E-qV_{oc}}{kTc}}-1} dE}{J_{SC}} \tag{20}$$

where $\overline{\mathrm{EQE}}$ is the appropriately weighted value over all angles of incident light. For textured cells, it is close to the near perpendicular value of the commonly measured EQE [31]. Eqs. (15), (18) and (19) provide a simple relation between the dominant contribution to the cell temperature sensitivity and the cell External Radiative Efficiency. Making the rough approximations of neglecting the ERE and the bandgap temperature dependences, we show in Fig. 9 approximated temperature coefficients as a function of cell bandgap for different EREs. This gives an idea of the evolution of TCs as cells improve towards the radiative limit. For illustration, crosses show experimental values of β_{Voc} for record efficiency crystalline silicon cells over the years. Diamonds show values measured on cells made of GaAs, GaSb and Ge [34]. One should not deduce ERE values directly from this graph because the approximations used can have an important impact on β_{Voc}. This is illustrated in Fig. 10 where β_{Voc} is calculated with different temperature dependences of the ERE and the bandgap. One can observe that different values of γ, i.e. different dERE/dT due to differences in dominant recombination mechanisms, lead to significant variations of β_{Voc}. Thus the knowledge of the ERE at 25 °C alone is not sufficient to accurately predict β_{Voc}. In opposition to a conclusion derived elsewhere [21], dE_g/dT is found to have an important impact on β_{Voc} because it relates E_g (25 °C) to E_{g0}. For example, assuming γ=1, the open circuit voltage temperature coefficients of $CsSnI_3$ and InP are respectively −583 and −1320 ppm K^{-1} while their bandgaps at 25 °C are similar (1.316

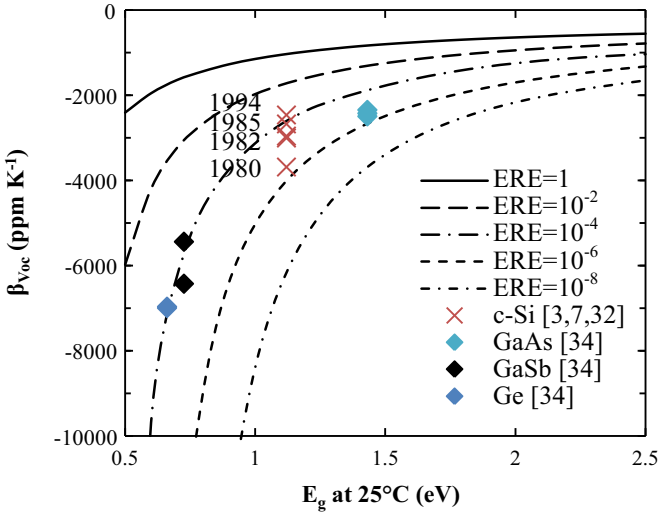

Fig. 9. Temperature coefficient of open circuit voltage as a function of bandgap for several external radiative efficiencies. From Eqs. (15), (18) and (19); dE_g/dT and $dERE/dT$ were neglected in the calculation (their importance can be seen in Fig. 10). The crosses are experimental values of β_{Voc} for some record efficiency c-Si cells over the years. The diamonds are experimental values of β_{Voc} for GaAs, GaSb and Ge cells.

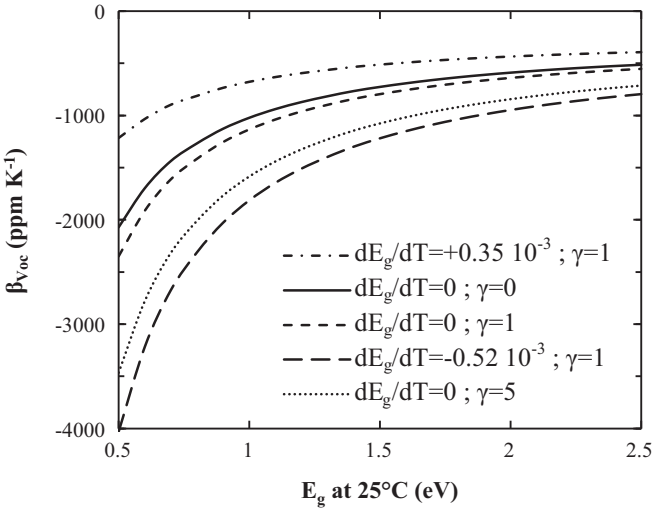

Fig. 10. Temperature coefficient of open circuit voltage as a function of bandgap from Eqs. (15), (18) and (19) for $ERE=1$ and different values of dE_g/dT and γ.

and 1.309 eV, respectively). Their overall TCs are not so far apart (Fig. 6) because the short circuit current TC of InP is positive while that of $CsSnI_3$ is negative because of the unusual behavior of its bandgap.

3.2. Short circuit current temperature sensitivity

Since most semiconductor bandgaps decrease with temperature (Fig. 4), the short circuit current density of solar cell (J_{sc}) generally increases with temperature. J_{sc} can be expressed as the product of an ideal current $J_{sc,1sun}$ and a collection fraction f_c [10] and potentially a concentration factor X:

$$J_{sc} = J_{sc,1sun} X f_c \tag{21}$$

The ideal current is determined by the photon flux density (PFD) of the incident radiation, the cell bandgap and its temperature dependence:

$$J_{sc,1sun} = q \int_{E_g(T_c)}^{\infty} \mathrm{PFD}(E)\, dE \tag{22}$$

As in Ref. [10], the temperature coefficient of the short circuit current can be written as

$$\beta_{Jsc} = \frac{1}{J_{sc}}\frac{dJ_{sc}}{dT_c} = \frac{1}{J_{sc,1sun}}\frac{dJ_{sc,1sun}}{dE_g}\frac{dE_g}{dT_c} + \frac{1}{f_c}\frac{df_c}{dT_c} \tag{23}$$

Note that the collection fraction (f_c) depends on reflection, transmission and parasitic absorption (especially by free carriers) of the cell. It is noteworthy that its variation with temperature differs between direct and indirect gap materials because phonons play a notable role in the interband absorption of the latter. Similarly to concentration, the effect of non-ideal absorption can easily be included in Eqs. (15) and (19) through the collection fraction f_c. However in practice its impact on β_{Voc} is negligible and thus was not included in the previous section.

Eqs. (22) and (23) indicate that β_{Jsc} depends on the incident spectral intensity at wavelengths near the bandgap. Fig. 11 shows the photon flux density of the reference AM1.5 spectrum [27] and of a solar simulator [35] together with the bandgaps of several semiconductors at 0 and 100 °C. While the average intensity of the solar simulator is close to that of the reference spectrum, the photon flux density is quite different. As previously noted elsewhere [6], this explains the scattering of β_{Jsc} values found in the literature. Even for indoor measurements, the spectral intensity distributions vary because of differences between solar simulators (even of the same type). This stresses the complexity of accurately predicting β_{Jsc} under real operating conditions, where the incident spectrum changes with time.

Fig. 11 shows that some semiconductor bandgaps lie near important fluctuations in the the AM1.5 photon flux density caused by the atmoshpere absorption. This creates non linearity in the temperature dependence of J_{sc} as illustrated in Fig. 12 for crystalline silicon. To represent the local variations of J_{sc}, a local temperature coefficient (in ppm K^{-1}) is defined as

$$\beta_{G\_loc}(T_c) = \frac{10^6}{G(298.15\ \mathrm{K})}\frac{G(T_c+1) - G(T_c-1)}{2} \tag{24}$$

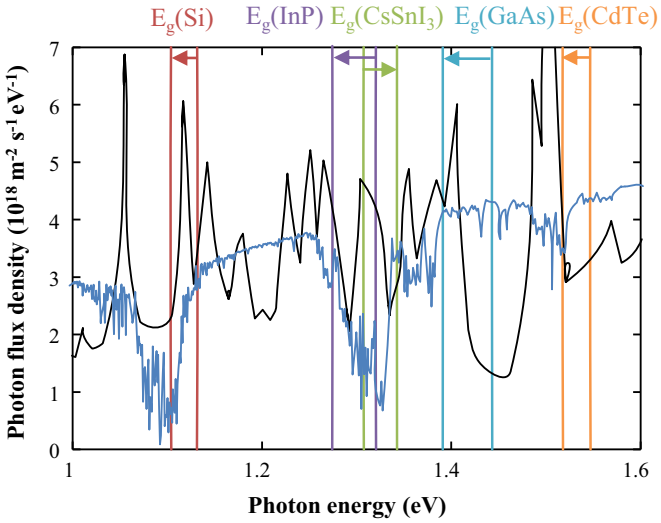

Fig. 11. Photon flux density of the AM1.5 reference spectrum (in blue), of a solar simulator [35] (in black). Bandgaps of different semiconductors at 0 and 100 °C; arrows show the direction of increasing temperature. (For interpretation of the references to color in this figure legend, the reader is referred to the web version of this article.)

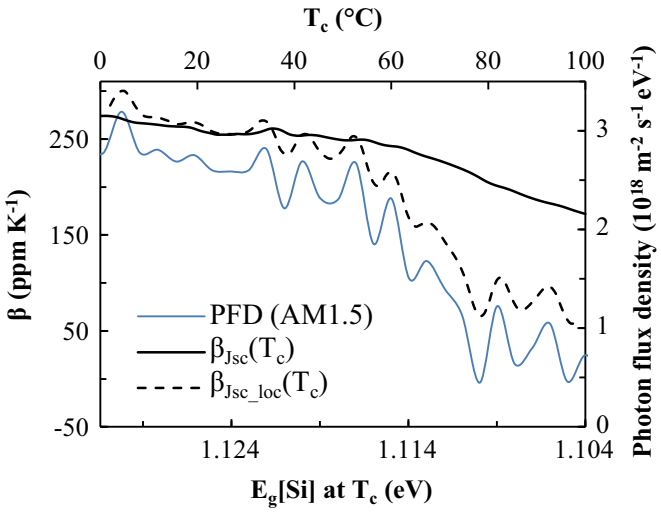

Fig. 12. Global (solid black line) and local (dotted black line) temperature coefficients of the short circuit current density of a c-Si cell with ideal light collection ($f_c=1$) and photon flux density of the AM1.5 reference spectrum (blue line). (For interpretation of the references to color in this figure legend, the reader is referred to the web version of this article.)

3.3. Fill factor temperature sensitivity

The fill factor (*FF*) relates the maximum power that can be extracted from a cell to its open circuit voltage (V_{oc}) and short circuit current (J_{sc}). It indicates the minimal "cost" of extracting the photogenerated charges from the cell into the circuit and corresponds to the optimal current/voltage trade-off. This optimum depends on the generation–recombination balance (similarly to V_{oc}) but also on the transport losses due to the current flow through the circuit at the maximum power point (MPP). This appears in the expression derived in Ref. [7]:

$$\frac{1}{FF}\frac{d\,FF}{d\,T} = (1 - 1.02\,FF_0)\left(\frac{1}{V_{oc}}\frac{d\,V_{oc}}{d\,T} - \frac{1}{T}\right) - \frac{R_s}{V_{oc}/I_{sc} - R_s}\left(\frac{1}{R_s}\frac{d\,R_s}{d\,T}\right) \quad (25)$$

$$FF_0 = \frac{v_{oc} - \ln(v_{oc} + 0.72)}{v_{oc} + 1} \quad (26)$$

$$v_{oc} = \frac{q}{nkT}V_{oc} \quad (27)$$

FF_0, R_s, and n, are respectively the ideal fill factor, the cell series resistance and the diode ideality factor. For good quality crystalline silicon cells, β_{FF} is mainly function of β_{Voc} and can be described by a simpler expression (Eq. (25) with R_s=0). In less-developed technologies, the fill factor temperature sensitivity is more complex. For example, in some amorphous silicon and nanocrystalline dye cells, the fill factor increases with temperature due to decreasing resistance effects or increasing "mobility-lifetime" products [10]. It is noteworthy that resistance effects are expected to increase with irradiance as the current circulating through the cell increases [36].

A concrete example of the complexity of fill factor temperature sensitivity is given in a recent paper by Deceglie et al. [12]. The temperature coefficient of the fill factor of some CIGS modules was found to be modified after light soaking. It was suggested that this is due to a light induced reduction in the conduction band offset between the buffer and the absorber. Since the charge transfer mechanisms across this barrier (tunneling or thermionic emission) are enhanced at high temperature, this metastable change could explain the observed variation of β_{FF}. This understanding is important because it is the final light soaked temperature coefficients that need to be known to model field performances.

4. Conclusion

Physics ruling the temperature sensitivity of solar cells has been presented and discussed. Dependences with temperature of the fundamental losses for single junction solar cells have been examined and fundamental temperature coefficients have been calculated. Impacts on temperature coefficients of the incident spectrum and of variations with temperature of the bandgap have been highlighted. It has been shown that the unusual behavior of the bandgaps of perovskite semiconductor compounds such as $CH_3NH_3PbI_{3-x}Cl_x$ and $CsSnI_3$ will ultimately, in the radiative limit, give PV cells made of these materials peculiar temperature sensitivities.

The different losses limiting the efficiency of present commercial cells have been depicted on a p–n junction diagram. This representation provides valuable information on the energy transfer mechanisms within PV cells. In particular, it has been shown that an important fraction of the heat generation occurs at the junction.

A review of the loss mechanisms driving the temperature coefficients of the different cell parameters (V_{oc}, J_{sc}, *FF*) has been proposed. The temperature sensitivity of open circuit voltage is connected to the balance between generation and recombination of carriers and its variation with temperature. A general expression that relates the temperature sensitivity of a cell V_{oc} to the cell quality measured by its External Radiative Efficiency (ERE) has been proposed. Knowing the ERE at room temperature enables to estimate the temperature coefficient of open circuit voltage β_{Voc}. However, the knowledge of the ERE dependence on temperature which is function of the dominant recombination mechanisms is required to predict the exact value of β_{Voc}.

The influence of bandgap temperature dependence and incident spectrum on the temperature sensitivity of short circuit current has been demonstrated. The temperature coefficient of short circuit current also depends on the collection fraction of incident photons; this can be particularly important for indirect bandgap semiconductors whose absorptivity increases with temperature.

Ideally, the fill factor temperature sensitivity is closely related to the open circuit voltage of the cell. In practice, it also depends on technological issues linked to carrier transport such as contact resistances. As demonstrated in a recent publication [12], it is still possible to improve the understanding of fill factor sensitivity of thin film solar cells.

The investigation of the fundamental causes for the temperature sensitivity of solar cells presented in this paper could be extended to any kind of radiative energy conversion (e.g. thermophotovoltaic concepts). As the industry is naturally evolving towards design of PV modules specific to certain location/conditions [37], opportunities for specific optimizations are likely to appear. The complete understanding of temperature behavior of PV modules might be a key towards such new optimizations.

Acknowledgments

Olivier Dupré is thankful to the School of Photovoltaic and Renewable Energy at the University of New South Wales that hosted him during six months and provided extended access to its library resources. He also acknowledges the doctoral school MEGA of Lyon for supporting the travel costs. The authors would also like to thank Gerald Siefer for providing experimental data. ACAP is supported by the Australian Government through the Australian Renewable Energy Agency (ARENA).

References

[1] J.J. Wysocki, P. Rappaport, Effect of temperature on photovoltaic solar energy conversion, J. Appl. Phys. 31 (1960) 571–578.
[2] M.A. Green, Solar Cells: Operating Principles, Technology, and System Applications, Prentice-Hall, Englewood Cliffs, NJ, 1982.
[3] M.A. Green, K. Emery, A.W.W. Blakers, Silicon solar cells with reduced temperature sensitivity, Electron. Lett. 18 (1982) 97–98. http://dx.doi.org/10.1049/el:19820066.
[4] J. Fan, Theoretical temperature dependence of solar cell parameters, Sol. Cells 17 (1986) 309–315.
[5] S. Nann, K. Emery, Spectral effects on PV-device rating, Sol. Energy Mater. Sol. Cells 27 (1992) 189–216. http://dx.doi.org/10.1016/0927-0248(92)90083-2.
[6] G. Landis, Review of solar cell temperature coefficients for space, in: Proceedings of the 13th Space Photovoltaic Research Technology Conference, 1994, pp. 385–399.
[7] J. Zhao, A. Wang, S.J. Robinson, M.A. Green, Reduced temperature coefficients for recent high performance silicon solar cells, Prog. Photovolt. Res. Appl. 2 (1994) 221–225. http://dx.doi.org/10.1002/pip.4670020305.
[8] S. Yoon, V. Garboushian, Reduced temperature dependence of high-concentration photovoltaic solar cell open-circuit voltage (V_{oc}) at high concentration levels, in: Proceedings of the IEEE 1st World Conference on Photovoltaic Energy Conversion – WCPEC (A Jt. Conf. PVSC, PVSEC and PSEC), 90505, 1994, pp. 1500–1504.
[9] D.J. Friedman, Modelling of tandem cell temperature coefficients, in: Proceedings of the Twenty Fifth IEEE Photovoltaic Specialists Conference – 1996, IEEE, 1996, pp. 89–92. doi:10.1109/PVSC.1996.563954.
[10] M.A. Green, General temperature dependence of solar cell performance and implications for device modelling, Prog. Photovolt. Res. Appl. 11 (2003) 333–340. http://dx.doi.org/10.1002/pip.496.

[11] G. Siefer, A.W. Bett, Analysis of temperature coefficients for III–V multi-junction concentrator cells, Prog. Photovolt. Res. Appl. 22 (5) (2012) 515–524. http://dx.doi.org/10.1002/pip.2285, n/a–n/a.
[12] M.G. Deceglie, T.J. Silverman, B. Marion, S.R. Kurtz, Metastable changes to the temperature coefficients of thin-film photovoltaic modules, in: Proceedings of the 40th Photovoltaic Specialists Conference (PVSC), IEEE, Honolulu, HI, 2014, pp. 337–340. doi:10.1109/PVSC.2014.6924926.
[13] L.C. Hirst, N.J. Ekins-daukes, Fundamental losses in solar cells, Prog. Photovolt. Res. Appl. 19 (2011) 286–293. http://dx.doi.org/10.1002/pip.1024.
[14] P.T. Landsberg, V. Badescu, Carnot factor in solar cell efficiencies, J. Phys. D Appl. Phys. 33 (2000) 3004–3008. http://dx.doi.org/10.1088/0022-3727/33/22/320.
[15] M.A. Green, Third generation photovoltaics: ultra-high conversion efficiency at low cost, Prog. Photovolt. Res. Appl. 9 (2001) 123–135. http://dx.doi.org/10.1002/pip.360.
[16] W. Shockley, H.J. Queisser, Detailed balance limit of efficiency of p–n junction solar cells, J. Appl. Phys. 32 (1961) 510–519. http://dx.doi.org/10.1063/1.1736034.
[17] P. Wurfel, The chemical potential of radiation, J. Phys. C Solid State Phys. 15 (1982) 3967–3985. http://dx.doi.org/10.1088/0022-3719/15/18/012.
[18] W. Ruppel, P. Wurfel, Upper limit for the conversion of solar energy, IEEE Trans. Electron. Devices 27 (1980) 877–882. http://dx.doi.org/10.1109/T-ED.1980.19950.
[19] P.F. Baldasaro, J.E. Raynolds, G.W. Charache, D.M. DePoy, C.T. Ballinger, T. Donovan, et al., Thermodynamic analysis of thermophotovoltaic efficiency and power density tradeoffs, J. Appl. Phys. 89 (2001) 3319–3327. http://dx.doi.org/10.1063/1.1344580.
[20] K. Emery, J. Burdick, Y. Caiyem, D. Dunlavy, H. Field, B. Kroposki, et al., Temperature dependence of photovoltaic cells, modules and systems, in: Proceedings of the 25th (PVSC), Photovoltaic Specialists Conference, IEEE, 1996, pp. 1275–1278. doi:10.1109/PVSC.1996.564365.
[21] A. Braun, E.A. Katz, J.M. Gordon, Basic aspects of the temperature coefficients of concentrator solar cell performance parameters, Prog. Photovolt. Res. Appl. 21 (2012) 1087–1094. http://dx.doi.org/10.1002/pip.2210.
[22] P. Dey, J. Paul, J. Bylsma, D. Karaiskaj, J.M. Luther, M.C. Beard, et al., Origin of the temperature dependence of the band gap of PbS and PbSe quantum dots, Solid State Commun. 165 (2013) 49–54. http://dx.doi.org/10.1016/j.ssc.2013.04.022.
[23] C. Yu, Z. Chen, J.J. Wang, W. Pfenninger, N. Vockic, J.T. Kenney, et al., Temperature dependence of the band gap of perovskite semiconductor compound $CsSnI_3$, J. Appl. Phys. 110 (2011) 063526. http://dx.doi.org/10.1063/1.3638699.
[24] K. Wu, A. Bera, C. Ma, Y. Du, Y. Yang, L. Li, et al., Temperature-dependent excitonic photoluminescence of hybrid organometal halide perovskite films, Phys. Chem. Chem. Phys. 16 (2014) 22476–22481. http://dx.doi.org/10.1039/C4CP03573A.
[25] P. Singh, N.M. Ravindra, Temperature dependence of solar cell performance—an analysis, Sol. Energy Mater. Sol. Cells 101 (2012) 36–45. http://dx.doi.org/10.1016/j.solmat.2012.02.019.
[26] M.A. Green, Intrinsic concentration, effective densities of states, and effective mass in silicon, J. Appl. Phys. 67 (1990) 2944–2954. http://dx.doi.org/10.1063/1.345414.
[27] Photovoltaic Devices—Part 3: Measurement principles for terrestrial photovoltaic (PV) solar devices with reference spectral irradiance data, International Standard, IEC 60904-3, 2nd ed., 2008.
[28] A. Olkhovets, R.C. Hsu, A. Lipovskii, F. Wise, Size-dependent temperature variation of the energy gap in lead–salt quantum dots, Phys. Rev. Lett. 81 (1998) 3539–3542. http://dx.doi.org/10.1103/PhysRevLett.81.3539.
[29] A. Richter, M. Hermle, S.W. Glunz, Reassessment of the limiting efficiency for crystalline silicon solar cells, IEEE J. Photovolt. 3 (2013) 1184–1191. http://dx.doi.org/10.1109/JPHOTOV.2013.2270351.
[30] S.C. Baker-Finch, K.R. McIntosh, A freeware program for precise optical analysis of the front surface of a solar cell, in: Proceedings of the 35th Photovoltaic Specialists Conference (PVSC), IEEE, 2010, pp. 2184–2187. doi:10.1109/PVSC.2010.5616132.
[31] M.A. Green, Radiative efficiency of state of the art photovoltaic cells, Prog. Photovolt. Res. Appl. 20 (2012) 472–476. http://dx.doi.org/10.1002/pip.
[32] M.A. Green, A.W. Blakers, C.R. Osterwald, Characterization of high-efficiency silicon solar cells, J. Appl. Phys. 58 (1985) 4402. http://dx.doi.org/10.1063/1.336286.
[33] U. Rau, Reciprocity relation between photovoltaic quantum efficiency and electroluminescent emission of solar cells, Phys. Rev. B 76 (2007) 085303. http://dx.doi.org/10.1103/PhysRevB.76.085303.
[34] G. Siefer, P. Abbott, C. Baur, T. Schlegl, A. Bett, Determination of the temperature coefficients of various III–V solar cells, in: Proceedings of the 20th European Photovoltaic Solar Energy Conference, Barcelona, Spain, 2005, pp. 495–498.
[35] K. Emery, Photovoltaic test performance: laboratory test procedures measure photovoltaic cells and modules according to international standards, Photonics Spectra 42 (2008) 76–80.
[36] H. Helmers, M. Schachtner, A.W. Bett, Influence of temperature and irradiance on triple-junction solar subcells, Sol. Energy Mater. Sol. Cells 116 (2013) 144–152. http://dx.doi.org/10.1016/j.solmat.2013.03.039.
[37] S. Kurtz, J. Wohlgemuth, P. Hacke, N. Bosco, M. Kempe, R. Smith, et al., The challenge to move from one size fits all to pv modules the customer needs, in: Proceedings of the 26th European Photovoltaic Solar Energy Conference, 2011, pp. 3064–3068.